Heliyon 9 (2023) e19394

Contents lists available at ScienceDirect

Heliyon

journal homepage: www.cell.com/heliyon

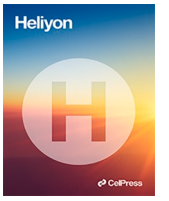

Stress dynamics associated with the Nyasa / Malawi rift: Implication for the present-day East African Rift System dynamics

Athanas S. Macheyeki [a,b,*], Hassan Mdala [c]

[a] Department of Geology, College of Earth Sciences and Engineering, the University of Dodoma, Tanzania
[b] Earth Sciences Institute of Shinyanga, P. O. Box 1016, Shinyanga, Tanzania
[c] Geological Survey Department of Malawi, Regional Office North, Pvt Bag 9, Mzuzu, Malawi

ARTICLE INFO

Keywords:
Nyasa
Malawi rift
East African rift system
Stress dynamics
Oblique transtensive rifting
Radial extension
Stress perturbation

ABSTRACT

The Nyasa/Malawi rift (NMR), known for its poor magma and notable seismic activity, has sparked a debate regarding its stress kinematics. It is on one hand viewed as a transform fault, while on other hand as a rift structure characterized by normal faulting. In order to address this controversy, we conducted paleostress analysis that involved collecting fault slip data along the central to southern region of the rift. We integrated our findings with published kinematic data on focal mechanisms in the rift. Our results reveal that the central part of the rift experiences radial or sub-radial extension, while the southern half is subject to oblique NNE-SSW transtensive tectonic forces. The minimum horizontal principal stress axis aligns with an orientation of 020°. As we move further south, the extension direction changes by approximately 25°, resulting in a predominantly north-south opening with a minimum horizontal stress axis direction of 175° (Shmin = 175°). The degree of structural penetration and intensity of faulting indicate that the north-south opening is more significant and pronounced in the southern region compared to the northern region. Additionally, we observed that faults dipping to the east and trending NW-SE exhibit sinistral (left-lateral) movement, while faults dipping to the southwestern side display dextral (right-lateral) movement. This suggests that, regionally, the NMR primarily experiences a normal faulting regime, albeit with a significant strike-slip component, which accounts for the oblique kinematics observed. The tectonic regimes identified through our fault slip data encompass the crust and upper mantle, spanning a lithospheric scale.

1. Introduction

There are various models of rifting, major ones attest to active rifting and passive rifting [1–3]. In the first case magma is the source of rifting whereby underlying magma heats the bottom of the lithosphere causing it to expand and consequently thin away and eventually rifting occurs [1,4,5]. In the second case, rifting takes place without involvement of magma [6,7]. In the latter case therefore, rifting is caused by far-field stresses. There are times where both models of rifting operate [8,9].

The East African Rift System (EARS) is one of such lithospheric scale structures where rifting occurs through both active and passive models [1,3].

In the process of rifting, earthquakes of various sizes occur depending on the source of the driving stresses and the magnitude (s) of

* Corresponding author. Department of Geology, College of Earth Sciences and Engineering, the University of Dodoma, Tanzania.
E-mail address: asmacheyeki@yahoo.com (A.S. Macheyeki).

https://doi.org/10.1016/j.heliyon.2023.e19394
Received 16 February 2023; Received in revised form 21 August 2023; Accepted 21 August 2023
Available online 24 August 2023

the same. The largest recorded earthquakes in rift systems are in little excess of Mw 7 [10]. In the EARS, the largest earthquake Mw 7.4, struck the western branch of the EARS in SW Tanzania (Rukwa area) on December 1910 [11] - though Midzi and Manzunzu [12] consider it to have been Mw 7.3. It did not cause large damage at that time because most of the houses were wooden made and were

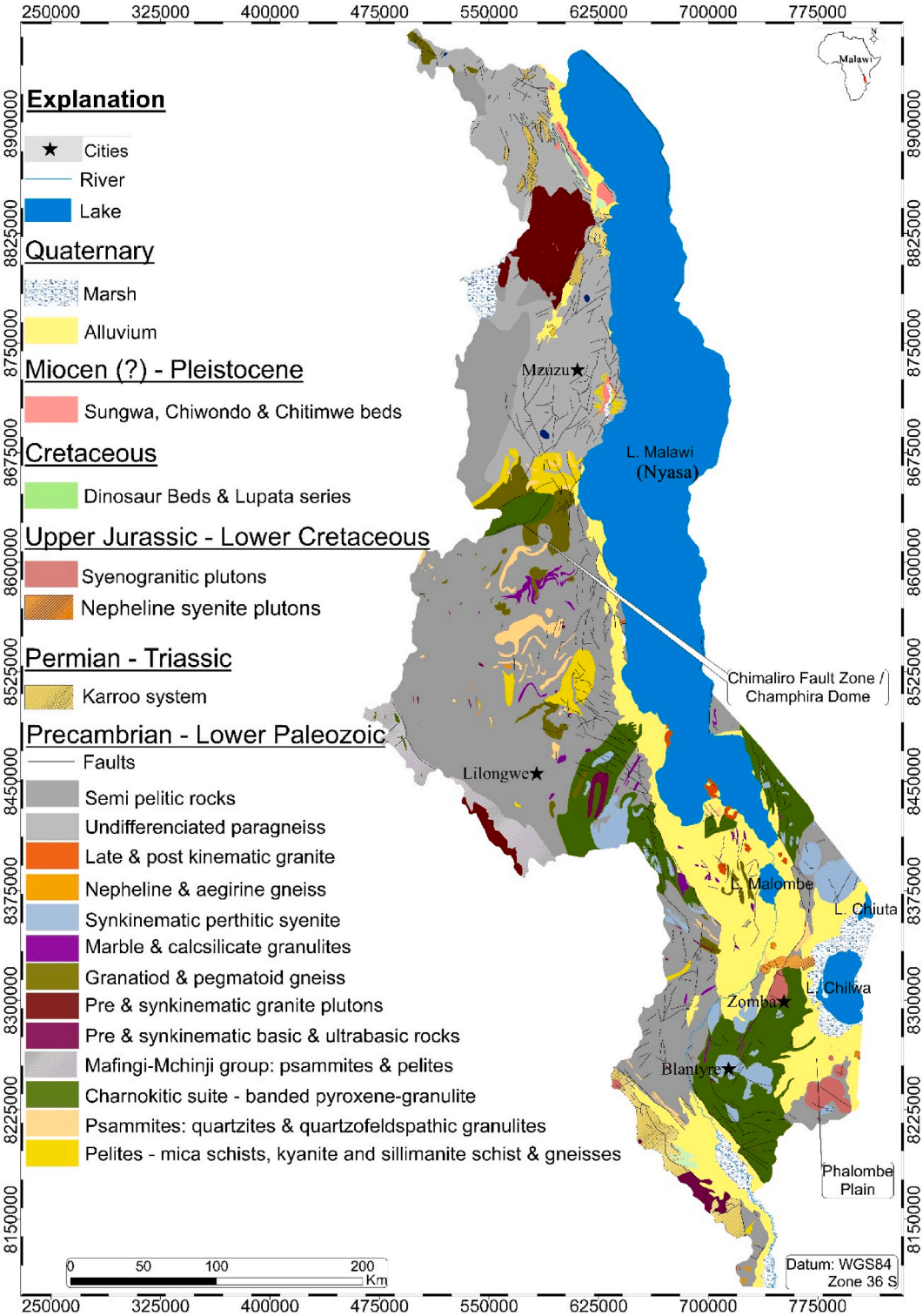

Fig. 1. Geological map of Malawi (modified from Ref. [23]).

scattered owing to a small population in that area at that time. Another earthquake in that order (Ms = 7.2) occurred on 20th May 1990 in Sudan (an area considered to be the 350 km extension of the EARS) [13]. The largest earthquakes within the Nyasa/Malawi rift (NMR) was in March 1989 (Mw = 6.1) and December 2009 (Mw = 6.0) in Salima and Karonga respectively [14,15]. While the NMR (Fig. 1) is considered to be part of the western branch of the EARS it is in part associated with magmatism in its northern part, the Rungwe volcanic province. This northern part of the NMR is considered to be associated with magma/mantle plume below [16]. The central and southern parts of the NMR are magma poor [16,17]. While the northern part of the NMR trends NNW-SSE, the central and southern parts of the NMR trend almost N–S and NW-SE respectively with local variations. Kinematics of rifting of the NMR is debatable to-date [17,18]. Chorowicz [19] for example considers the NMR to be like a part of southern segment of the 2100 km long western branch of the EARS. Further, Chorowiciz [19] considers the NMR to be part of the Tanganyika-Rukwa-Malawi fault zone that connects two main segments of the western branch. Ebinger [17] examined local earthquakes and analyzed source mechanisms from teleseismic events to challenge the prevailing notion of NW-SE transform faulting in the NMR. Their findings demonstrate an extension direction of NE-SW, specifically oriented towards N58°E and N65°E. Similar works in support of the NE-SW extension of the northern NMR are by Refs. [18,20–22]. These controversies in the rifting kinematics of NMR is the main motivation for this research work.

1.1. Regional structural geological setting

The NMR is predominantly underlain by Precambrian to Lower Paleozoic Basement Complex rocks [23,24] (Fig. 1). Across Malawi, three mobile belts, namely the Ubendian, Irumide and Mozambique belts, have affected the Lower Paleozoic Basement Complex rocks. According to Ref. [23], these three mobile belts are associated with two distinct tectono-metamorphic events. The first event involved the Paleoproterozoic Ubendian mobile belt causing plastic deformation of the Basement Complex rocks. The second event involved both the Meso-Proterozoic Irumide and the Neo-Proterozoic Mozambique belts, which caused brittle deformation of the Basement Complex rocks. In the Northern Province of Malawi, the dominant rocks are from the Ubendian and Mozambique belts, while in the Southern Province, the Mozambique and Irumide mobile belts are prevalent [23].

The Basement Complex rocks are overlain by sedimentary rocks of the Karroo System, which have an age range from Permian to Upper Triassic or Lower Jurassic. These Karroo sedimentary rocks are primarily prevalent in the northern region of the country,

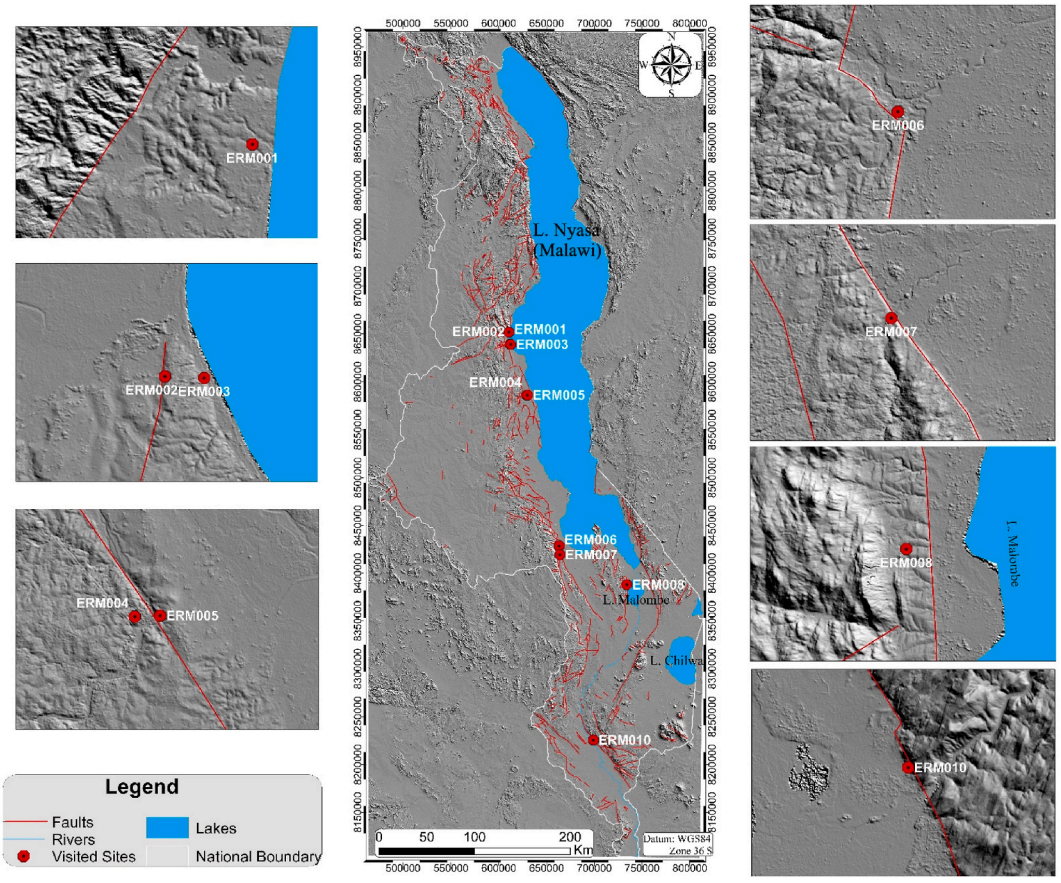

Fig. 2. Visited sites in Malawi. The Central panel shows the localities of the sites at a regional scale whereas the panels on the left and right are giving closer view of the studied area (sites) in 3D of 30m-resolution SRTM-DEM data. Traces of the rift are shown as solid red lines.

although some occurrences can also be found in the southern part [23] (Fig. 1).

The Karroo rocks are overlain by the Chilwa Alkaline Province rocks, which consist of syeno-granitic and nepheline syenite plutons, volcanic vents and carbonatites. These rocks are of Upper Jurassic to Lower Cretaceous age. Following the Chilwa Alkaline rocks, there is a succession of sedimentary rocks from the Cretaceous, Pleistocene and Quaternary periods (Fig. 1). These sedimentary rocks can be observed in the northern part of Malawi, central Malawi, and the southwestern side of Blantyre in southern Malawi [23,25].

Tertiary and Quaternary deposits, comprising of alluvium and colluvium sediments are the last in the succession. They are mostly found aligned in a narrow belt parallel to the NMR and along the Lilongwe-Kasungu plains in the central region of Malawi and the Phalombe plain to the southern end of Lake Chilwa. The Recent volcanics from the Rungwe volcanic province characterize the northern Malawi [18]. In these areas, most of the Basement Complex structures are obscured by thick layers of residual cover.

[23,25] describe tectonic structures of Malawi to be divided into two age groups namely Pre-Cenozoic and Cenozoic structures. The Pre-Cenozoic structures mainly faults, shear zones and dyke swarms are believed to have formed during the Permian to Triassic Karroo rifting ca. ~280 to 195 Ma and Post Karroo rifting of Jurassic to Cretaceous period (~195–65 Ma). The Chimaliro fault zone which is to the southern side of the Champhira dome is an example of a Pre-Cenozoic structure (Fig. 1).

The second group of structures comprises those structures which were formed during the Cenozoic age, which in Malawi started about 10 million years ago during the initiation of the EARS in this area [26]. The general orientations of the rift related structures in both Northern and Southern Provinces of Malawi are NW-SE and N–S with minor NE-SW trending pattern. This, according to Delvaux [18] is a clear indication that the present orientation of the rift related structures is a reflection of the orogenic related structures of the Ubendian, Mozambique and Irumide mobile belts, implying possible reactivation. Owing to its Z-like shaped, right-stepped pattern (Figs. 1 and 2), the NMR appears to be made of several rift segments.

2. Material and methods

Between October and November 2022, an extensive fieldwork campaign was conducted along the NMR, covering a distance of

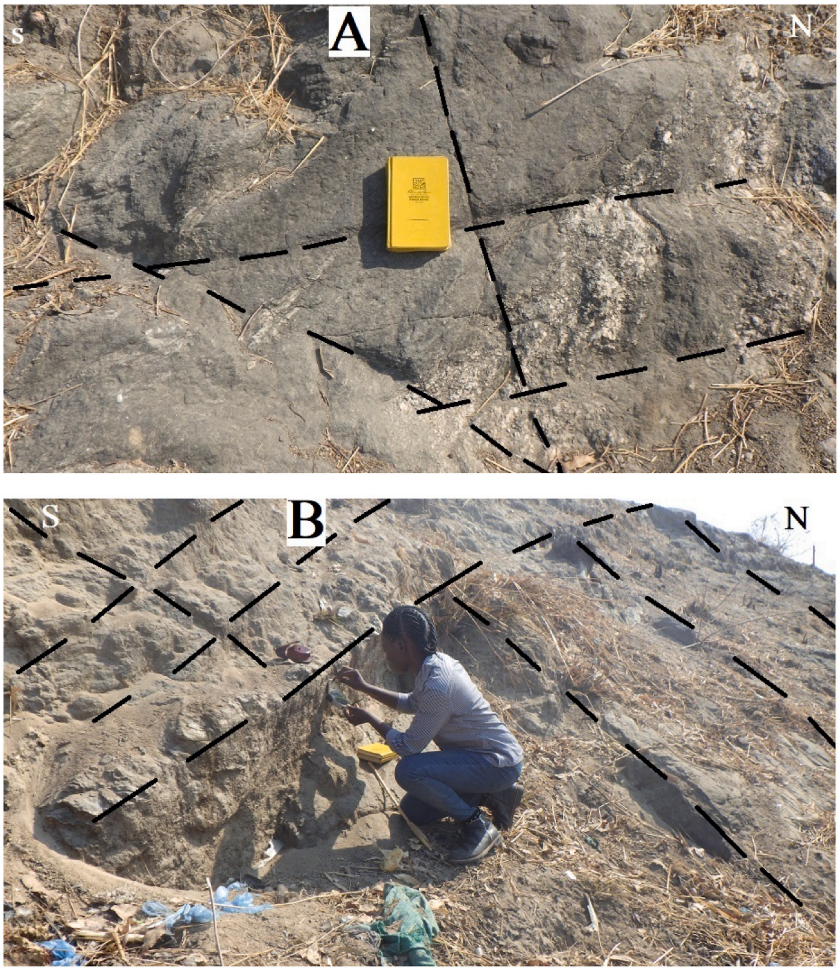

Fig. 3. Active faults at Kasitu village, ERM02: (A)- Sub-orthogonal and non-orthogonal conjugate faults, (B) - Orthogonal active conjugate faults.

approximately 450 km from its central to southern regions. The primary objective of this study was to unravel the complex sequence of stress regimes and determine the underlying kinematics within the NMR. To achieve this, focal mechanism data from Ebinger [17] were utilized to model the present-day stress field and kinematics and compare it with modelled stress regime from fault slip data that were collected in this field campaign. In the field, measurements were made on fault planes, both with and without slickensides, including the determination of dip amount, dip direction, plunge amount and plunge directions. Fault planes without slickensides were classified as fracture planes or joints, while those with slickensides were considered as fundamental planes for determination of stress regime type and kinematics of the same. Relative ages of faulting events on fault surfaces were established based on the presence of minerals, mineral types and cross-cutting relationships between minerals and slickensides. Various types of slickensides encountered

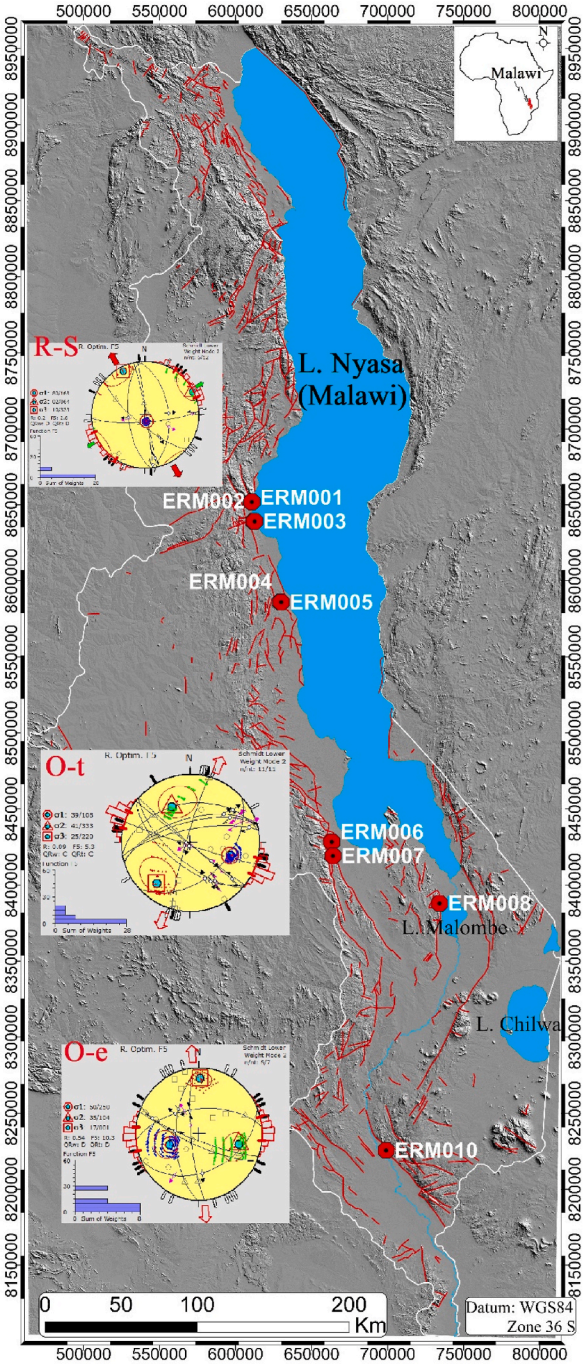

Fig. 4. –Modelled stress regime from fault slip-data (paleostress analysis) plotted on google earth snapshot. R–S = Radial to sub-radial extensive, O-t = Oblique transtensive (NNE-SSW), O-e = Oblique extensive (N–S). For coordinates of sites visited see Fig. 2. Compare with Table 1.

Table 1
Stress tensor parameters obtained from fault slip data for the NMR. (n): number of data used in the inversion, (nt): total number of data in the database, (σ_1, σ_2 and σ_3) are the principal stress axes, i.e. maximum, intermediate and minimum respectively, (R): stress ratio, (QRw): quality rank, (R′): stress regime index, (Reg): stress regime according to the World Stress Map, (SHmax, Shmin): respectively, maximum and minimum horizontal principal stress directions. (σ mag): normal stress magnitude, (τ mag): shear stress magnitude and (Θ) the angle between normal and shear stress.

Site ID	Location	n	nt	σ_1	σ_2	σ_3	R	R'	SHmax	Shmin	Regime	Stress Regime	Θ	σ mag	τ mag	QRw
ERM002/3	Kasitu A/B	6	12	80/168	02/064	10/333	0.2	0.2	61	151	NF	Radial EXTENSIVE	24.8	30.4	16	D
ERM006	Kazipuru river	11	11	39/108	41/333	25/220	0.09	1.91	110	20	NS	Oblique TRANSTENSIVE	38.5	37.7	31.7	C
ERM010	Thabwa-(Thyolo Fault)	6	7	50/250	35/104	17/001	0.54	0.54	85	175	NS	Oblique EXTENSIVE	35.7	42.5	26.8	D

include Riedel shears, mineral steps, and conjugate shear fractures. Once the data and information were collected, they were entered into the Win-Tensor software developed by Damien Delvaux and processed using the procedures outlined in Delvaux and Sperner [27]. Field raw data were compiled in Supplementary Table 1a, b, c.

A total of ten geological sites, designated as ERM001 to ERM010, were visited and designated. However, it's worth noting that no fault slip data were recorded at Site ERM009. To facilitate model creation, data from eight specific locations—namely ERM002 to ERM008 and ERM010 (as indicated in Fig. 2)—were included in the analysis. Site ERM001 had insufficient data to be utilized in the modeling process and was consequently excluded. For the processing and modeling of fault slip data, the Win Tensor software was employed. This software necessitates a minimum of four fault slip data points. Unfortunately, Site ERM001 did not meet this requirement, leading to its exclusion from the modeling phase. Nevertheless, even though the data from Site ERM001 were not integrated into the modeling, a comparative analysis was carried out against data from nearby sites, namely ERM002 and ERM003 (refer to Fig. 2). Furthermore, during the data processing, a grouping approach was adopted based on geographical proximity. Specifically, ERM002 and ERM003, both situated near Kasitu village, were grouped together. Similarly, due to their close proximity, ERM004 and ERM005 were also grouped together.

Sites ERM002 and ERM003 are located at Kasitu village: Both sites are within a few hundred meters and are just on the western lake shore (Fig. 2) and about 120 km by road south of Mzuzu City (the Northern Administrative Headquarter of the Northern Region of Malawi). Sites ERM004 and ERM005, near Diwangu and Bua rivers (Fig. 2) are located along the lake shore, about 60 km south of the Kasitu sites. The other important site is the Kazipuru river bridge (Site ERM006): This site is located on the southern part of the NMR (Fig. 2). About 10 km south of Kazipuru river is the Mua site, ERM007 (Fig. 2). Nearly 80 km SE of this site is the Malombe site (Site ERM008). It is located just east of the Malombe fault and west of Lake Malombe. The last site is the Twabwa Quarry: site ERM010: This site is more than 200 km by road south of ERM008.

3. Results

The Kasitu A and B, i.e. sites ERM002 and ERM003 portray three structural orientations; NNW-SSE, N–S and NNE-SSW. Large number of the structures are fresh-looking high-angle faults (mainly conjugated joints or shear fractures), typically cross-cutting each other at approximately $\leq 60^{\circ}$. Some shear fractures cross-cut each other orthogonally or nearly so (Fig. 3A and B).

Further, detailed investigation at both sites indicate presence of (a) sub-vertical planes with dip amounts between 75° and 88°, associated with sub-horizontal slip-lines $<20^{\circ}$, typically 6° to 19°. These slip-lines indicate both sinistral and dextral shear movements-they are interpreted as strike-slip fault planes; (b) planes dipping between 54° and 68°: Most of these fault planes are conjugated and oriented NW-SE. They are interpreted as normal fault planes indicating rift opening in an ENE-WSW; and (c) shallow – angle dipping planes (approximately 40°): These fault planes are oriented NE-SW. Direction of movement in one of the slip lines on these fault planes is NE-SW (i.e. 39° towards 028°). These types of faults are showing oblique opening along NE-SW, sub-parallel to the orientation of the fault planes themselves.

It can be summarized from these sites that opening of the rift at both Kasitu A and B is ENE-WSW and NE-SW regardless of the type of structures in which the movement is occurring. Modelled stress tensor for these sites indicate normal faulting regime with radial extension stress regime characterized by Shmin = 151°, SHmax = 061° (Fig. 4, Table 1).

Unlike the Kasitu sites that are characterized by three main fault trends, the ERM004 and ERM005 sites are characterized by only two main fault trends; NW-SE and NNW-SSE. The main fault planes are high-angle faults, typical of strike-slip faults and are oriented in such a way that those faults that dip to the east and trending NW-SE (or NNW-SSE) are characterized by sinistral sense of movement whereas those that dip to the southwestern side (in the same trend), are characterized by dextral sense of movement (Fig. 6). Foliation fabric of the Precambrian basement measured here dips 40° towards 220°.

Site ERM006 is characterized by NW-SE trending faults which are the major ones here. NE-SW trending faults are also present but comparably less pronounced than the former. There are also W-E trending faults. While field relationship show that all the three sets of faults are relatively younger (i.e. Cenozoic), the W-E trending faults seem to be the youngest owing to their fresher surfaces and they occur as echelon structures, typical of isolated fault strands. The E-W faults are however, less penetrative, probably restricted to the upper crust.

In the same site are E-W trending thrust faults. Their planes of movement are associated with quart-hornblende minerals implying that they are the oldest faults or are among the oldest structures in the area. The overall stress field from modelled stress tensor corresponding to the present stress kinematics is shown in Fig. 4. It is characterized by an oblique transtensive stress field oriented NNE-SSW with Shmin = 020°, SHmax = 110°.

The Mua site, ERM007 (Figs. 2 and 6) is characterized by a fresh cut of a normal fault scarp associated with water falls indicating recent faulting. Most of the faults here are high-angle dipping faults implying that the normal fault related scarp was formed from reactivation of strike-slip faults. Few measurements taken at this point indicate that the fault planes dip between 68° and 74° and the slip lines show block movements directed 40° dip amount towards 336° (NW).

Like for most fault planes in the central to southern Malawi, the fault planes at the Malombe site (Site ERM008) are mostly high-angle (dipping approximately 70° to sub-vertical) and generally dipping to the north and NNE (Fig. 7A). The prominent structures at Malombe site are the WNW-ESE fault planes that dip due north to NNE. Slip vectors along the fault planes vary from N to E, meaning that there are faults that open in a N–S direction and those that open in an E-W direction. The latter are less prominent whereas the faults that open in a N–S direction are prominent (Fig. 7A) and are more deep seated or penetrative than at Kazipuru site (ERM006).

On the western side of the Malombe site where the Malombe fault is located, lies clear landslide (Fig. 7B). This landslide has affected most of the rock units in the area and has equally disturbed the orientation of some of the structures on this hanging wall side

including the structures at the Malombe site (ERM008).

Site ERM010 (Twabwa Quarry) is along the NW-SE trending Thyolo active fault (Figs. 2 and 8). Both dip slip and lateral movements characterize any given fault plane in this locality. The prominent sense of movement in all the faults in this southern most part of the rift is sinistral. Three types of faults are recognized from their planes and slip vectors; normal, strike-slip and thrust faults. The latter is quartz veined and therefore relatively older than the normal and strike slip faults (the barren ones). The oldest tectonic structures in the area are the S–C fabrics associated with Precambrian deformational events. The modelled stress tensor corresponding to the most recent rifting stress field is presented in Fig. 3. It indicates that this southernmost part of the NMR is opening obliquely along the N–S direction. Comparing site ERM006, ERM008 and ERM010 in terms of level of N–S opening slickensides, it is evident that the magnitude is increasing southerly. The slickensides within the fault planes are clearer as one moves from central part of the NMR to the southern part (i.e. from ERM006 to ERM08).

4. Discussion

According to Daly [28], the NW-SE trending Precambrian Ubendian structures are ductile to semi-ductile shear zones and folds. These are intersected by NE-SW trending Karoo shear zones, normal and strike-slip faults [16]. The zones of intersections were, and are still the weakest structural zones and future locus for fault reactivation and deep seated magmatism of the EARS.

Observations from Site ERM006 show pervasive brittle deformation exemplified by fault breccia, most likely related to Karoo rifting. The thrust faults are also attributed the Karoo tectonics. In the same area are tight folds, characterized by NNW-SSE trending axial planes. These ductile-semi ductile structures seem to have been formed by NNE-SSW compressive stress field. In summary, field relationship indicates that possible sequence of tectonic events in the area are as follows: (a) metamorphism of the Precambrian basement, (b) folding of the basement, (c) thrusting associated with quartz-hornblende mineralization/and faulting (as indicated by fault breccia), (d) recent deformation associated with the barren faults (strike slip and normal faults)-of all these the E-W faults are related to Cenozoic rifting (Fig. 5A and B).

[16,20] show that the Cenozoic rifting reactivated Precambrian structures (shear zones). According to Delvaux [20], the reactivation in Late Miocene to Pleistocene was a near radial extensive regime and was followed by strike-slip faulting (compressive regime) in the Late Pleistocene. Both the Late Miocene-Pleistocene and the Late Pleistocene tectonic events were associated with the magmatic pulses in the Rungwe volcanic province.

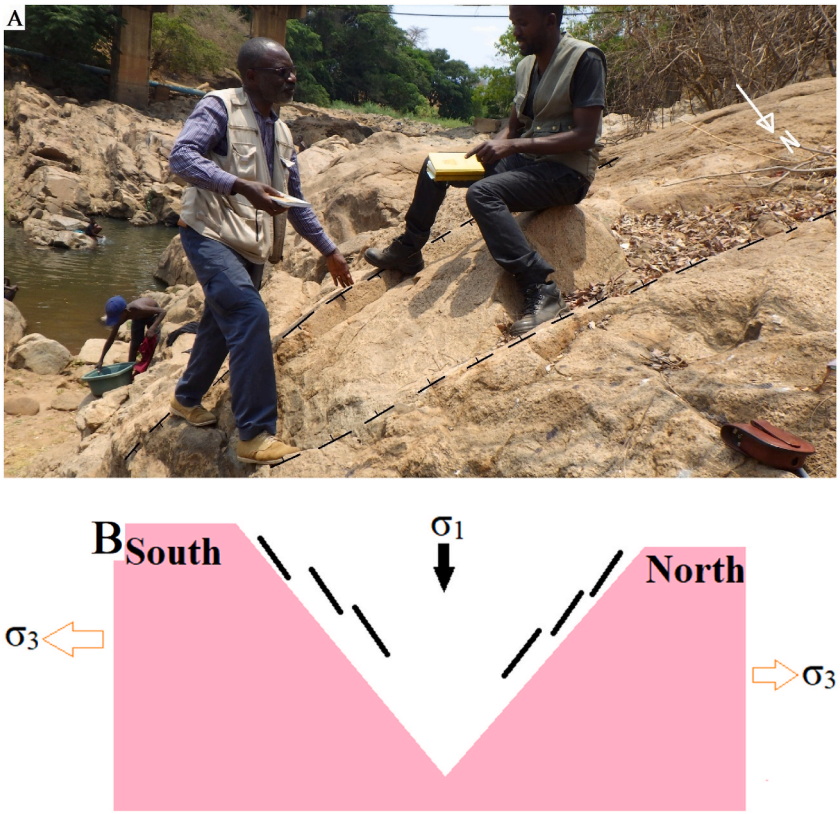

Fig. 5. A – E-W trending echelon faults at Kazipuru river bridge (indicated by dashed thick lines). Thin lines point to the dip direction of block movement (i.e. movement direction of the grabben). Fig. 5B- Conceptualized model of the E-W echelon faults at Kazipuru river bridge. Compare with similar structures in Fig. 7A.

Fig. 6. The Mua site (ERM07) water fall 10 km south of Kazipuru river (site ERM06). Note the freshness of the fault scarp at this point indicating active faulting in the area. Photo taken facing west.

This work has demonstrated five major findings: that the central part is under radial extension. This is compatible with the Late Miocene - Pleistocene rifting model reported by Ref. [20] for the northern part of the NMR. Such results indicate that the radial extension is from the central part to the northern part of the rift. Radial extension means opening of the rift in all directions-a phenomenon that is attributed to plume activities or lithospheric scale magmatic activities [29]. One of the evidences for multiple opening directions is at Kisitu village (ER002 and ERM003) where movement of blocks is both towards the northern and eastern directions (Compare with Fig. 4).

The other finding is that southern half of the NMR is under oblique NNE-SSW transtensive tectonic regime with Shmin = 020°. Another finding from this study is that further south, the obliquity extension rotates by about 25° reaching N–S direction with Shmin = 175° (Table 1, Fig. 3). Type localities for this N–S extension phenomena were recorded in Kazipuru river (ERM006, Fig. 5A and B), Malombe fault (west of Lake Malombe, ERM008, Fig. 7A) and Twabwa area along the Thyolo fault (ERM010, Fig. 8A–D). Apart from the N–S extension in the Tholo fault, we also observe sinistral strike-slip faulting (Fig. 8D) oriented sub-parallel to the direction of the Thyolo fault.

Further, the level of structural penetration and intensity of faulting show that the N–S opening is more pronounced in the south than towards the north and finally, the faults that dip to the east and trending NW-SE are characterized by sinistral sense of movement whereas those that dip to the SW side are characterized by dextral sense of movements (Fig. 9). It implies that the rift is essentially under normal faulting regime but with a significant strike –slip component – hence the obliquity kinematics.

As most of the data collected on the Malawi side indicate that fault planes dipping to the eastern side have sinistral sense of movement as contrasted by the fault planes dipping to the western side which have dextral sense of movement, it implies that most of the faults in Malawi (i.e. middle and southern part) that dip towards the eastern side are under sinistral oblique faulting and the faults in the northern segment that dip to the west are under dextral sense of movements.

Focal mechanism solutions for the northern and central Malawi compiled by Ebinger [17] for small to moderate earthquakes that occurred in the last half a century (1968–2019) consistently indicate overall extension in a NE direction, typically 65°. The stress regime being normal faulting and oblique faulting and involve seismogenic layer of up to 35 km with little difference between ~100- and 120-km-long border faults and ≤30 km-long intrabasinal normal faults.

Putting both fault slip and focal mechanism data into a regional perspective, it can be deduced that, the NMR has not been deforming in the same way both in time and space. During the Late Pleistocene, the lithospheric scale deformation assisted by mantle plume, affected the middle to northern part of the rift which is a relatively magma rich in the NMR causing it to open radially. This explains why the middle/central part of the NMR are under radial extension. Delvaux [20] also report radial extension regime in the northern NMR related to Miocene – Pleistocene Epochs. It means that this event continued to the Late Pleistocene Epoch or even to Holocene Epoch. During the same time (Late Pleistocene to Holocene), the southern part is opening obliquely under the so called oblique NNE-SSW transtensive regime and further to the southern end, it is opening in an oblique N–S extensive regime.

It is though difficult to comprehend a N–S extension within a generally N–S oriented NMR. Owing to freshness of the N–S opening structures (Figs. 5, 7 and 8) and the relatively less penetrative field relationship, it can be implied that these structures are related to upper crust deformation process (s) which are related to secondary faults [30] and are developed by local stress perturbations [30–32]

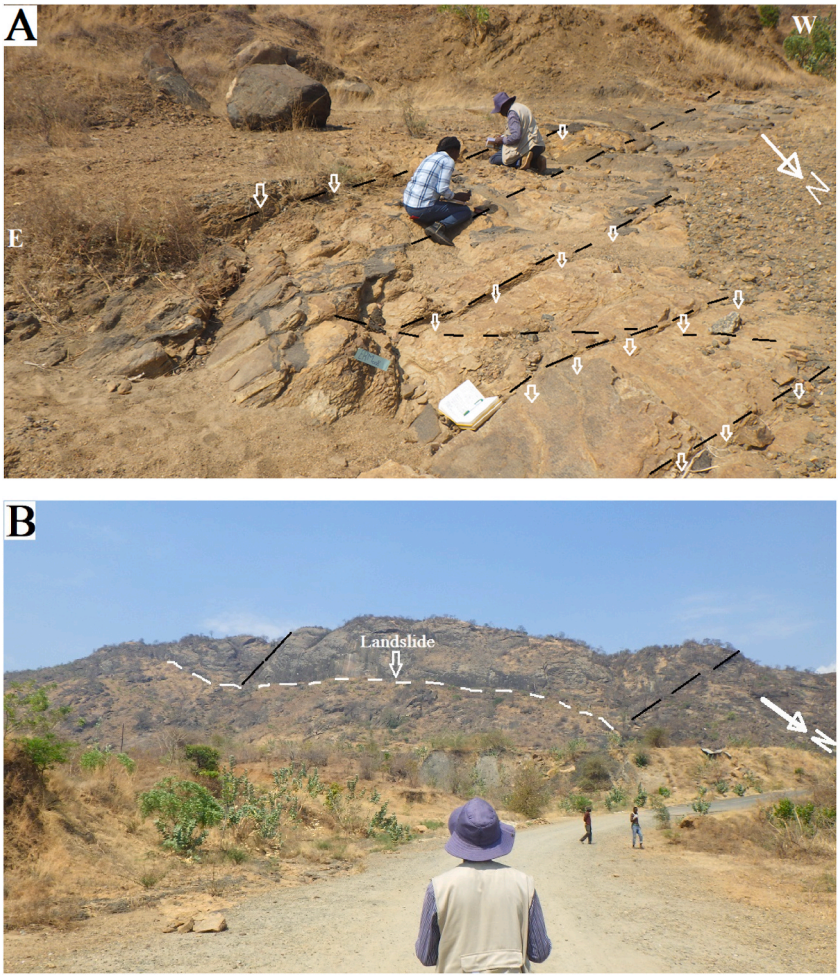

Fig. 7. (A). East -West trending faults at Malombe site, block movements towards the north (ERM08). (B). Landslide west of Malombe site. Note the directions of movement of blocks in 'A' and 'B' are shown by open arrows. Black dashed lines indicate trace of active faults. E = East W = West. Person facing landslide is standing at Malombe site (Fig. 7A).

in the process of rifting caused by active/and far field stresses. Stress perturbations, and hence changes of positions of the principal stress axis σ_1 can occur as a result of pre- and post-seismic stress states differences [32–34] and pore pressure changes [35]. As the NMR is still a younger rift and more particularly towards its southern tip, it is not surprising to find these intra basinal structures that are sub-orthogonal to the rift being developed (e.g. Fig. 5A and B) and are more important towards the southern (relatively youngest) tip of the rift (Fig. 8).

5. Conclusion

The northern to central part of the NMR is under radial to sub-radial extension because of both tectonic and possibly magma activities. The southern part of the rift is opening obliquely in the NNE-SSW to N–S. The latter kinematics is considered to be attributed to stress perturbations at the upper crustal level - the process that is actively ongoing in the NMR. Therefore, the actual active regional opening direction of the NMR to its southern part, hereby reported is NNE-SSW characterized by an oblique transtensive stress field with Shmin = 020° and $R' = 1.91$ meaning that faulting/rifting has both normal and strike-slip components. This NNE-SSW extensional direction for the NMR obtained from this work is in disagreement with some of the published extensional directions that attests to NE-SW directions [17], extension direction N58°E and N65°E) and NW-SE [19,36].

Additionally, we observed that faults dipping to the east and trending NW-SE exhibit sinistral (left-lateral) movement, while faults dipping to the southwestern side display dextral (right-lateral) movement. This suggests that, regionally, the NMR is primarily under a normal faulting regime (less likely a transform fault or part of it), albeit with a significant strike-slip component, which accounts for the oblique kinematics observed. The tectonic regimes identified through our fault slip data encompass the crust and upper mantle, spanning a lithospheric scale. More studies are proposed to unveil in detail the interplay between stress field changes and magma dynamics below the crust in the NMR.

Fig. 8. A- Oblique normal faults opening N–S at Thyolo fault (Site ERM010). Their displacements are larger than those in Sites ERM006 and ERM008, over 200 km north of ERM010; (B) – A zoom in of 8A; (C) - Conjugate fault system at Thyolo fault, the kinematics of which indicate that σ_3 (the Principal stress axis of minimum compression or maximum extension) is oriented almost N–S (i.e. obtuse angle subtended by the conjugate faults); and (D) – Sinistral strike-slip fault (blue and pink dotted lines represent two different quartz veins offset by the NW-SE trending rift related sinistral strike-slip fault).

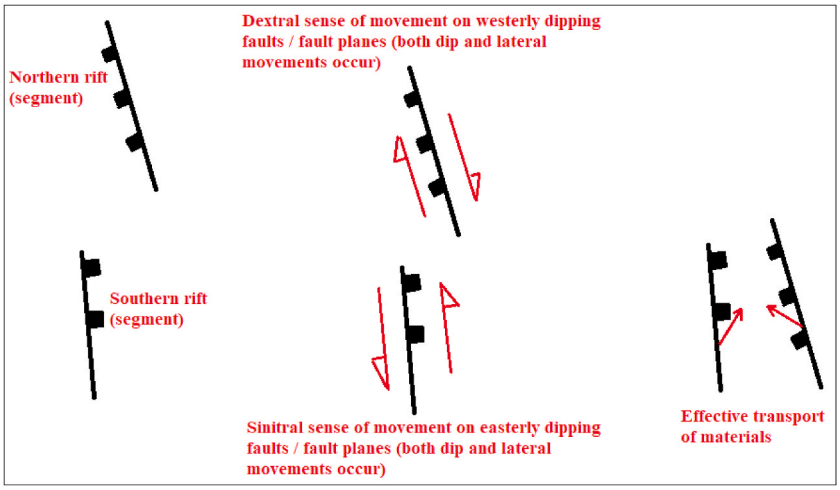

Fig. 9. Conceptual model of fault (rift) orientations along with sense of movement in Malawi. Type locality of the conceptual model is Diwangu and Bua rivers (ERM04).

Author contribution statement

Athanas S. Macheyeki: Conceived and designed the analysis; Analyzed and interpreted the data; Contributed analysis tools or data; Wrote the paper.

Hassan Mdala: Analyzed and interpreted the data; Contributed analysis tools or data; Wrote the paper.

Data availability statement

Data included in article/supplementary material/referenced in article.

Declaration of competing interest

The authors declare that they have no known competing financial interests or personal relationships that could have appeared to influence the work reported in this paper.

Acknowledgements

This mission was made possible through the warm collaboration between the Geological Survey Department of Malawi (MGSD). We particularly thank Mr. Kondwani Dombola, the Acting Director of the MGSD for accepting the request of the first author to work with the Survey. The MGSD made available to the researchers, the resources such as data, field vehicle and organized for field logistics throughout the time we were in Malawi. We are indebted to Mr. Patrick Chindandali and Mr Yohane Kaukutu (Librarian) both from MGSD for making available to us some literatures useful for our work. Special thanks to Rebeka B. Mwakalinga from Tanzania for her technical assistance in the field. Mr Benjamin Chirwa provided a safe and warm driving throughout the fieldwork. We also thank each and every one who in one way or another supported us. Anonymous reviewers are highly thanked for their constructive comments that shaped the early versions of the manuscript. Some phrases in *Material and methods* section were refined using AI (GPT-3.5).

Appendix A. Supplementary data

Supplementary data related to this article can be found at https://doi.org/10.1016/j.heliyon.2023.e19394.

References

[1] M.H.P. Bott, Mechanisms of rifting: geodynamic modeling of continental rift systems, Dev. Geotecton. 25 (C) (1995) 27–43, https://doi.org/10.1016/S0419-0254(06)80006-6.
[2] C. Prodehl, K. Fuchs, J. Mechie, Seismic-refraction studies of the Afro-Arabian rift system - a brief review, Tectonophysics 278 (1–4) (1997) 1–13, https://doi.org/10.1016/S0040-1951(97)00091-7.
[3] G. Corti, M. Bonini, S. Conticelli, F. Innocenti, P. Manetti, D. Sokoutis, Analogue modelling of continental extension: a review focused on the relations between the patterns of deformation and the presence of magma, Earth-Science Rev. 63 (3–4) (2003) 169–247, https://doi.org/10.1016/S0012-8252(03)00035-7.
[4] W.R. Buck, Modes of continental lithospheric extension, J. Geophys. Res. 96 (B12) (1991) 161–178, https://doi.org/10.1029/91jb01485.
[5] F. Gueydan, J. Précigout, Modes of continental rifting as a function of ductile strain localization in the lithospheric mantle, Tectonophysics 612–613 (2014) 18–25, https://doi.org/10.1016/j.tecto.2013.11.029.
[6] M.H.P. Bott, Mechanisms of rifting: geodynamic modeling of continental rift systems, Dev. Geotecton. 27 (C) (2006) 27–43, https://doi.org/10.1016/s0419-0254(06)80006-6.
[7] H. Liu, et al., Relationships between tectonic activity and sedimentary source-to-sink system parameters in a lacustrine rift basin: a quantitative case study of the Huanghekou Depression (Bohai Bay Basin, E China), Basin Res. 32 (4) (2020) 587–612, https://doi.org/10.1111/bre.12374.
[8] S. Dumont, Y. Klinger, A. Socquet, C. Doubre, E. Jacques, Magma influence on propagation of normal faults: evidence from cumulative slip profiles along Dabbahu-Manda-Hararo rift segment (Afar, Ethiopia), J. Struct. Geol. 95 (2017) 48–59, https://doi.org/10.1016/j.jsg.2016.12.008.
[9] C.J. Ebinger, Recipe for Rifting: Flavors of East Africa, second ed., vol. 4, July. Elsevier Inc., 2020, https://doi.org/10.1016/B978-0-08-102908-4.00100-4.
[10] W.P. Yang, Z. Chen, Earthquakes along the East African Rift System: A Multiscale, System-wide Perspective, Geophysics, 2010, 790000, https://doi.org/10.1029/2009JB006779.
[11] N.N. Ambrassey, The rukwa earthquake of 13 december 1910 in east africa, Terra Nov 3 (2) (1991) 2020–2211, https://doi.org/10.1111/j.1365-3121.1991.tb00873.x.
[12] V. Midzi, B. Manzunzu, Large recorded earthquakes in sub–Saharan Africa, Extrem. Nat. Hazards, Disaster Risks Soc. Implic. 9781107033 (September 2016) (2012) 214–224, https://doi.org/10.1017/CBO9781139523905.020.
[13] R.W. Girdler, D.A. Mcconnell, R.W. Girdler, D.A. McConnell, April 1993 264 (1994) 1–4.
[14] J. Jackson, T. Blenkinsop, The Bilila-Mtakataka fault in Malawi: an active, 100-km long, normal fault segment in thick seismogenic crust, Feb, Tectonics 16 (1) (1997) 137–150, https://doi.org/10.1029/96TC02494.
[15] A.S. Macheyeki, et al., Active fault mapping in Karonga-Malawi after the December 19, 2009 Ms 6.2 seismic event, J. African Earth Sci. 102 (Feb. 2015) 233–246, https://doi.org/10.1016/j.jafrearsci.2014.10.010.
[16] E.A. Njinju, et al., Lithospheric Structure of the Malawi Rift: Implications for Magma-Poor Rifting Processes 38 (2019) 11, https://doi.org/10.1029/2019TC005549.
[17] C.J. Ebinger, et al., Kinematics of Active Deformation in the Malawi Rift and Rungwe Volcanic Province, Africa 20 (8) (2019), https://doi.org/10.1029/2019GC008354.
[18] D. Delvaux, The Karroo to Recent Rifting in the Western Branch of the East African Rift System: A Bibliographic Synthesis," Mus. Roy. Afr. centr., Tervuren (Belg, Dept. Geol. Min, 1991, pp. 63–83. Accessed: Aug. 14, 2014. [Online]. Available: http://faculty.ksu.edu.sa/geography-alsaleh/ILWIS/ilwis_user_guide30.pdf.
[19] J. Chorowicz, The East African Rift System, J. African Earth Sci. 43 (1–3) (Oct. 2005) 379–410, https://doi.org/10.1016/j.jafrearsci.2005.07.019.
[20] D. Delvaux, K. Levi, K. Kajara, S. Sarota, Cenozoic paleostress and kinematic evolution of the rukwa - north Malawi rift valley (east African Rift System), Bull. du Cent. Rech. elf Explor. Prod. elf Aquitaine 16 (2) (1992) 383–406.
[21] R.A. Morley, C. K, F.M. Karanja, W.A. Wescott, D.M. Stone, R.M. Harper, S.T. Wigger, Da, y, "Geology and Geophysics of the Western Turkana Basins, Kenya.," AAPG Stud. Geol. 44 (1999).
[22] A.S. Macheyeki, D. Delvaux, M. De Batist, A. Mruma, Fault kinematics and tectonic stress in the seismically active manyara-dodoma rift segment in Central Tanzania - implications for the east African Rift, J. African Earth Sci. 51 (4) (2008) 163–188, https://doi.org/10.1016/j.jafrearsci.2008.01.007.
[23] G.S. Carter, J.D. Bennet, Bulletin No 6, in: The Geology and Mineral Resources of Malawi, Malawi Geological Survey Library, Zomba, Malawi, 1973.
[24] G.E. Ray, The Geology of the chitipa - Karonga area, in: Bulletin No 42, Malawi Geological Survey Library, Zomba, Malawi., 1975. Accessed: Jul. 17, 2014. [Online]. Available: http://www.bgs.ac.uk/research/highlights/2010/malawiMineralPotential.html.
[25] L. Chapola, State of Stress in East and Southern Africa and Seismic Hazard Analysis of Malawi, Institute of Solid Earth Physics, University of Bergen, Norway (MSc Thesis)., 1997. Accessed: Oct. 13, 2014. [Online]. Available: http://www.researchgate.net/post/How_do_I_extract_lineaments_from_Landsat_Image_and_RADAR.

[26] A.S. Macheyeki, Present Day Faults Kinematics and Their Reactivation Likelihood within and South of the North Tanzania Divergence (NTD), East African Rift System: Implication for Geo-Hazards Assessment, J. Geol. Surv. India, 2023.
[27] D. Delvaux, B. Sperner, New aspects of tectonic stress inversion with reference to the TENSOR program, Geol. Soc. Spec. Publ. 212 (2003) 75–100, https://doi.org/10.1144/GSL.SP.2003.212.01.06.
[28] M.C. Daly, Crustal shear zones in central africa : a kinematic approach to proterozoic tectonics, Episodes 11 (1) (1988).
[29] M.C. Reiss, et al., The impact of complex volcanic plumbing on the nature of seismicity in the developing magmatic natron rift, Tanzania, Front. Earth Sci. 8 (2021), https://doi.org/10.3389/feart.2020.609805.
[30] D. Maerten, L. Gillespie, P. Pollard, "Effects of local stress perturbation on secondary fault development,", J. Struct. Geol. 24 (3) (2002) 145–153.
[31] Y.Z. Chen, X.Y. Lin, Z.X. Wang, T-stress evaluation for slightly curved crack using perturbation method, Int. J. Solids Struct. 45 (1) (2008) 211–224, https://doi.org/10.1016/j.ijsolstr.2007.07.020.
[32] Q. Feng, C. Yang, Y. Ma, X. Qi, B. Zhang, P. Meng, J. Tan, C. Chen, Local stress perturbations associated with the 2008 Wenchuan M 8.0 earthquake near the Longmenshan fault zone in the eastern margin of the Tibetan Plateau, J. Asian Earth Sci. 200 (2020), 8913181, https://doi.org/10.1016/j.jseaes.2020.104429.
[33] A. Hasegawa, K. Yoshida, Y. Asano, T. Okada, T. Iinuma, Y. Ito, Change in stress field after the 2011 great Tohoku-Oki earthquake, Earth Planet Sci. Lett. 355 (356) (2012) 231–243, https://doi.org/10.1016/j.epsl.2012.08.042.
[34] T. Yoshida, K. Hasegawa, A. Okada, T. Linuma, Changes in the stress field after the 2008 M 7.2 Iwate-Miyagi Nairiku earthquake, Geophys. Res. Solid Earth 119 (2014) 9016–9030.
[35] M. An, F. Zhang, E. Dontsov, D. Elsworth, H. Zhu, L. Zhao, Stress perturbation caused by multistage hydraulic fracturing: implications for deep fault reactivation, Int. J. Rock Mech. Min. Sci. 141 (September 2020) (2021), 104704, https://doi.org/10.1016/j.ijrmms.2021.104704.
[36] U. Ring, C. Betzler, Geology of the Malawi rift: kinematic and tectonosedimentary background to the chiwondo beds, northern Malawi, J. Hum. Evol. 28 (1) (1995) 7–21, https://doi.org/10.1006/jhev.1995.1003.